Indian Journal of Chemical Technology
Vol. 32, March 2025, pp. 203-210
DOI: 10.56042/ijct.v32i2.13942

Efficient degradation and mineralization of 4-nitrophenol achieved through innovative saponite-based Al-Ti pillared clay catalyst

Sudha Minz, Renu Gupta*, Baneesh Patial & Sangeeta Garg
Department of Chemical Engineering, Dr. B R Ambedkar National Institute of Technology, Jalandhar, Punjab-1440 08, India
*E-mail: bansalr@nitj.ac.in

Received 24 September 2024; accepted 7 February 2025

Pillared clay catalysts are emerging as heterogeneous catalysts for degrading refractory organic pollutants. The present study modified saponite clay using aluminium and saponite metal cations to synthesize Al-Ti pillared clay catalyst (Al-Ti PICC). It is subsequently used to study the degradation and mineralization of 4-nitrophenol. The synthesized Al-Ti saponite clay catalyst is characterized using XRD, BET isotherm, SEM, XRF, and thermo-gravimetric analysis. XRD, BET, XRD, and SEM characterization of Al-Ti PICC results indicate higher surface area (74 m^2/g), d-spacing (17 Å), porous and fluffy surface compared to saponite clay. The thermo-gravimetric study reveals a lower decomposition of Al-Ti PICC (5.7%) than saponite clay (38.7%). The parameters affecting the degradation and mineralization of 4-nitrophenol, such as H_2O_2 dosage, catalyst dose, and temperature, were optimized. At optimized conditions: 20 mM H_2O_2, 3 g/L of synthesized Al-Ti PICC, and 70°C at 5.7 pH 83.5% mineralization (Total organic carbon removal) with 95.6% degradation of 4-nitrophenol, was achieved after 240 min of reaction time. The TOC removal data was further used to study the reaction kinetics using the lumped kinetic model (LKM). It was observed that the data described well the LKM model for the mineralization of 4-nitrophenol.

Keywords: Al-Ti PICC, Degradation of 4-nitrophenol, Lumped kinetic model, Mineralization, Saponite clay

Introduction

Nowadays, advanced oxidation processes (AOPs) have emerged as a promising alternative to conventional methods (biological, chemical, and thermal treatment methods) for the treatment of refractory organic pollutants[1]. All the AOPs are based on the generation of highly reactive oxidizing hydroxyl radicals ($HO^{\bullet}$) and are very effective for the degradation of organic pollutants[2-6]. Among various AOPs like Fenton oxidation, photo-catalytic oxidation, electrocatalytic oxidation, ozonation, catalytic wet air oxidation, etc. The Fenton oxidation process has succeeded in decolorizing/degrading organic pollutants[7]. However, the Fenton oxidation process produces a large amount of iron sludge, which needs additional treatment for its disposal, which is effective for acidic medium only. The catalytic wet peroxide oxidation (CWPO) method among all AOPs has acquired the attention of researchers for its potency to degrade organic pollutants under mild temperature and pressure conditions and overwhelm the limitations of the homogeneous Fenton oxidation process[8-10]. Clays play an eminent function as a catalyst in the oxidation of organic pollutants by CWPO process[11]. The clay may be modified by pillarization to enhance the performance. The pillarization process comprises the intercalation of the cations present in the pillaring solution in the available space between interlayers of clay[12]. The literature has reported various metal cations pillared interlayered clay catalysts (PICCs) (Al-Fe PICCs, Al-Cu PICCs, Al-Zr PICCs, Al-Ce-Fe PICCs, Al-Cr PICCs) employed for the degradation of various organic pollutants. The studies of various authors showed complete decolorization/ degradation of reactive dyes, phenol, tyrosol, 4-CP, acid orange 7 dye, rhodamine B dye, and 4-Nitrophenol (4-NP)[13-17]. Daud and Hameed[18] reported 98.5% for decolorizing acid red 1 dye using Fe PICC. Zhou *et al.*[19] observed the complete removal of 4-CP using Al-Fe PICC. Ts *et al.*[20] showed 99% degradation of sulfanilamide using Al-Fe PICC onto montmorillonite clay. The COD removal was 84.26% of amoxicillin in a photo-assisted CWPO process with Al-Fe PICC[21], whereas it was 85% and 75% for rhodamine B and 4-NP[16]. TOC removal for wastewater containing olive oil was 80% and 75% using Cu-PICC and Fe-PICC[22]. Catrinescu *et al.*[13] and Zhou *et al.*[19] observed 60% and 72% TOC removal of 4-CP using Al-Fe PICC onto montmorillonite and bentonite clay, respectively. Herney-Ramirez[14] reported 70% TOC removal for acid orange 7 dye using Al-Fe PICC. Gao *et al.*[16] observed 40% and 80% TOC removal for rhodamine B dye and

4-NP, respectively. Al-Ti PICC has also been investigated as effective catalyst for degrading organic pollutants due to their high surface area and strong acidic sites[23].

The studies of Gao *et al.*[16], Ayodele *et al.*[21], Catrinescu *et al.* [24], and Bel[25] have reported the degradation of organic pollutants using PICCs and CWPO in the pH range of 5 to 7 and that they are stable against the leaching of metals. Due to the stability and workability of PICCs in the high pH range of 5 to 7, they have been considered as an effective catalyst for degradation of refractory organic pollutants using CWPO process.

In the present work, 4-NP has been chosen as the model pollutant as it has serious health effects on both humans and animals[26]. According to the US EPA, its maximum allowable concentration in the environmental matrix is 20 µg/L[27]. Various studies have been reported on CWPO using PICCs, but no work is available on the mineralization and degradation of 4-NP using saponite based Al-Ti Pillared clay catalyst. No studies are available yet on the kinetics based on total organic carbon removal histories for the degradation of 4-NP using Al-Ti PICC heterogeneous catalyst. In the present study, the mineralization (TOC removal) and degradation of 4-NP have been evaluated using Al-Ti PICC in the CWPO process. Effect of various parameters, such as the concentration of H_2O_2, the dose of Al-Ti PICC, and temperature on the degradation and mineralization (TOC and COD removal) of 4-NP, have been investigated. The work has been further extended to analyze the reaction kinetics based on the lumped kinetic model for the TOC removal histories of 4-NP using Al-Ti PICC.

Experimental Section

Reagents

Saponite clay (99% pure) was bought from Nanoshel (USA). 4-nitrophenol (98% w/w), $AlCl_3.6H_2O$ (99% pure), $TiCl_4$ (99.5% pure), and H_2SO_4 (98% pure) were procured from Loba Chemie (India). H_2O_2 (30% w/w) was procured from Ranbaxy Limited (India). NaOH (97% purity) and hydrochloric acid (35%) were purchased from SD Fine Chemical (India). Double distilled water was used to prepare the solutions.

Synthesis of Catalyst

Al-Ti PICC was synthesized with the co-intercalation method. Firstly, titanium tetrachloride ($TiCl_4$, 0.2 M) was mixed in 5 M HCl solution, then the chloride solutions of aluminum ($AlCl_3.6H_2O$, 0.1 M) and titanium ($TiCl_4$) were mixed in the molar ratio of 5:1 under continuous stirring and heated to 60°C. Thereafter, NaOH (0.2 M) solution was added dropwise to attain the molar ratio of $OH^-/(Al^{3+} + Ti^{4+})$ to 2. The resultant solution was kept at 60°C for 3 h and then it was cooled down to room temperature. 2wt% of saponite clay was dispersed in ethanol with continuous stirring for 24 h. The prepared saponite suspension was added dropwise into the above solution to achieve until the ratio of $(Al^{3+} + Ti^{4+})$/clay reached 10 mmol/g. The resultant solution was stirred continuously for another 3 h at 60°C. Further, the mixture was centrifuged to recover the solid and then washed with water. The solid was dried and calcined in a furnace at 500°C for 2 h[28].

Al-Ti PICC Characterization

X-ray diffraction patterns of samples were analyzed using an X'PERT-PRO diffractometer (PW3064, Philips Japan) with Cu–K-α radiations (λ = 1.54 Å). The scanning angle (2θ) was ranged from 3 to 50°. N_2 adsorption-desorption isotherms using Quantachrome, (USA) were carried out to measure the surface area and pore volume of saponite and Al-Ti PICC. SEM technique was carried out using JEOL (JSM 6510, Japan) to study the surface morphology of the saponite and Al-Ti PICC. The elemental composition of the samples was analyzed using X-ray fluorescence (S8 Tiger, Bruker, Germany). Thermogravimetric and Derivative Thermogravimetric (TG and DTG) studies of saponite and Al-Ti PICC were executed between room temperature and 1000°C using (EXSTAR TG-DTA 6300) with N_2 stream.

Catalytic performance of Al-Ti PICC

Al-Ti PICC (0.1 g) was added in 100 mL of 4-NP (100 ppm) in a temperature-controlled 250 mL reactor made of glass. The temperature of the mixture was maintained at 30°C, and the pH was 5.7. Initially, the mixture was stirred for 15 min, and the sample was taken out to study the adsorption of 4-nitrophenol onto the surface of the Al-PICC. Negligible adsorption was seen, and thereafter, 4 mM of H_2O_2 was added for the oxidation of 4-nitrophenol, and the reaction was carried out for 4 h. Reacted samples were drawn off from the reactor regularly after 10 min initially and latterly after 30 min. The reacted samples were filtered using filter paper and were analyzed immediately for degradation and TOC removal. Concentrations of 4-NP were examined at λ_{max} 318 nm for degradation (%) using UV/VIS spectrophotometer (Shimadzu, Japan). TOC

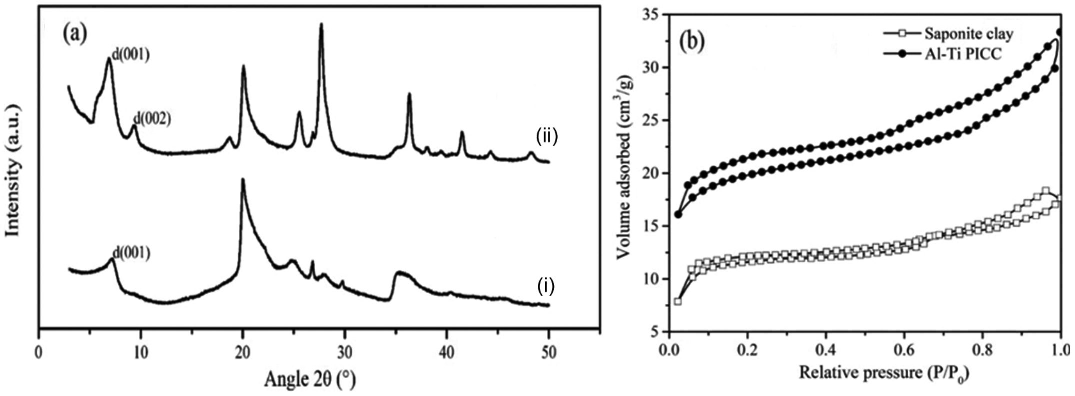

Fig. 1 — (a) XRD patterns (i) saponite clay, (ii) Al-Ti PICC and (b) BET isotherms for saponite clay and Al-Ti PICC

analysis was done by a non-dispersive infrared analyzer (TOC-V CPN, Shimadzu, Japan). The effect of various parameters was accessed by varying H_2O_2 concentration, catalyst dose, and temperature on degradation and mineralization of 4-NP. Experiments were repeated thrice to attain reproducibility within ±5%. The degradation and mineralization efficiencies (%) were calculated as:

$$\text{Degradation efficiency (\%)} = \frac{C_0 - C_t}{C_0} \text{ x } 100 \qquad \ldots (1)$$

Where, C_0 and C_t are the initial and final 4-NP concentrations, respectively.

$$\text{Mineralization efficiency (\%)} = \frac{TOC_0 - TOC_t}{TOC_0} \text{ x } 100 \qquad \ldots (2)$$

Where, TOC_0 and TOC_t are the initial and final total organic carbon contents, respectively.

Results and Discussion

Characterization of Al-Ti PICC

X- ray diffraction

XRD patterns of saponite and Al-Ti PICC are shown in Fig. 1(a). In saponite clay, the peak at 7.5° of 2θ represents basal spacing $d_{(001)}$ of 11.8 Å. Peaks at 21° and 26.5° show quartz impurity whereas at 29° it shows the presence of calcite[9, 17, 29]. After pillaring the saponite clay with Al-Ti metal cations, there is a slight shift in basal spacing towards the left side (Fig. 1a(i). The sharp peak at 2θ angle of 5.2° in Al-Ti PICC indicated an increase in $d_{(001)}$ of 17 Å. In Al-Ti PICC peak at 9.4° of 2θ angle shows basal spacing $d_{(002)}$ of 9.4 Å. The results are in accordance to the studies of Kaneko[30].

Table 1 — BET isotherm parameters for saponite and Al-Ti PICC catalyst

Catalyst	Surface area (m^2/g)	Pore volume (cm^3/g)	Pore diameter (Å)
Saponite	34	0.0043	5.1
Al-Ti PICC	74	0.0517	28.0

Surface area

N_2 adsorption-desorption curves of saponite clay and Al-Ti PICC are shown in Fig. 1(b) revealed the characteristic behaviour of layered materials with slit-like pores. The results are in accordance to the studies of Mata *et al.*[31]. Fig. 1(b) revealed a higher specific surface area for Al-Ti PICC (74 m^2/g) as compared to saponite clay (34 m^2/g). Also, Al-Ti PICC showed 12 and 5.5 times higher pore volume and 5.5 average pore diameter in comparison to saponite clay as shown as (Table 1).

Scanning electron microscope

The surface image of saponite clay and Al-Ti PICC is presented in Fig. 2(a). SEM image of the saponite clay expressed smooth and layered surface whereas for Al-Ti PICC the rough, porous, fluffy, and crystalline surface appears. The results indicate an increase in active sites for the Al-Ti PICC catalyst after pillaring it with Al and Ti metal cations and the results are in accordance to the studies of Guerra *et al.*[32].

Wavelength dispersive X-ray fluorescence

Chemical composition analysis of saponite and Al-Ti PICC was made to quantify the composition of various metal oxides present in saponite clay and Al-Ti-PICC and are listed in Table 2. It shows the decrease in the contents of oxides of silica whereas the oxides of aluminium and titanium increased significantly in Al-Ti PICC as compared to saponite

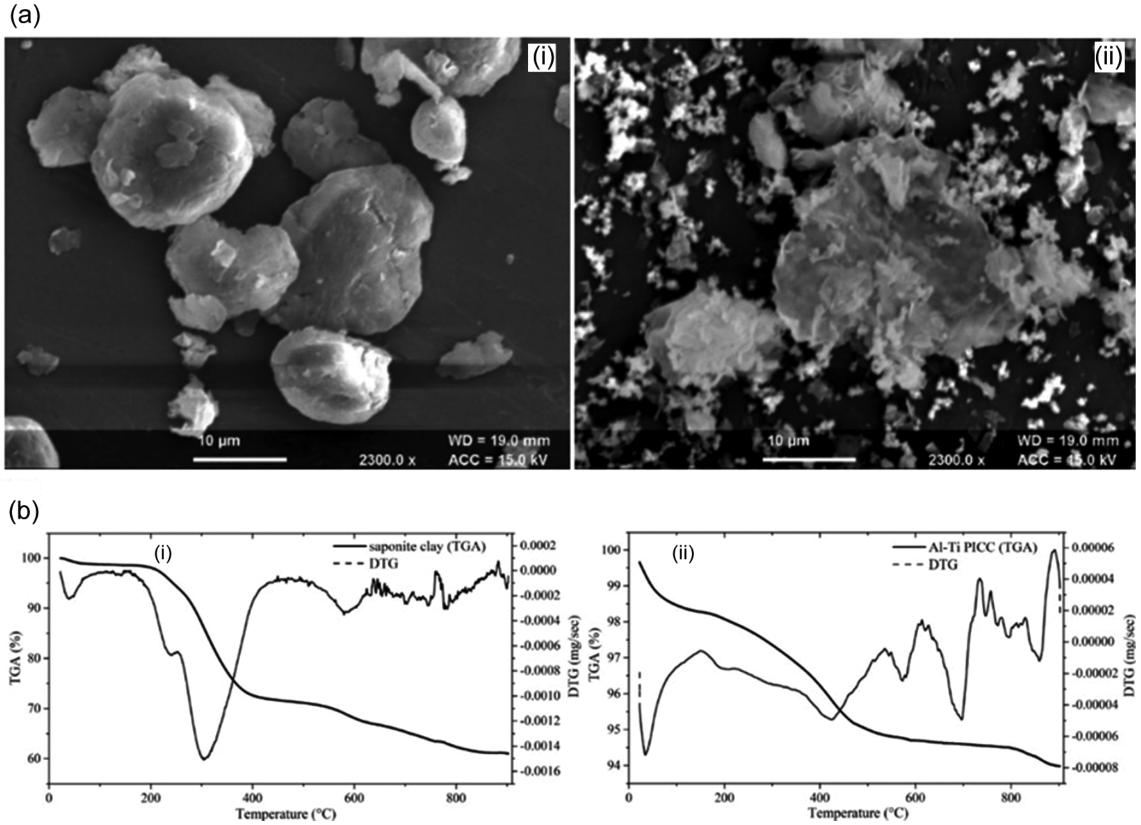

Fig. 2 — (a) SEM images (i) saponite, (ii) Al-Ti PICC and (b) TG/DTG curves (i) saponite clay, (ii) Al-Ti PICC

Table 2 — Chemical composition (wt%) for saponite and Al-Ti PICC catalysts

Catalyst	SiO_2	Al_2O_3	Fe_2O_3	K_2O	TiO_2
Saponite	65.4	15.9	1.3	1.3	0.2
Al-Ti PICC	21.2	28.9	2.4	-	21.4

clay. TiO_2 content in saponite clay was 0.2 (wt%) whereas in Al-Ti PICC, it was found to be 21.4 wt%. The results confirm the presence of Al and Ti metal cations in the synthesized Al-Ti PICC.

Thermogravimetric and Derivative thermogravimetric (TGA and DTG) Analysis

TA and DTG isotherms for saponite and Al-Ti PICC are presented in Fig. 2(b). TGA curves for saponite and Al-Ti PICC represented the three-stage weight loss below 1000°C. For saponite clay, in the first stage, the weight loss was 25.6% when the temperature was increased from 22°C to 200°C which was mainly due to loosely bound water molecules, whereas for Al-Ti PICC it was 1.6%. In the second stage at a temperature rise from 200°C to 800°C, the loss in weight for saponite clay was around 10.1% whereas for Al-Ti PICC it was 3.5%. In the third stage i.e. above 800°C the loss in weight was attributed to the structural hydroxyl group dehydration of the catalyst[33]. The third stage weight loss for saponite clay was 1.3% while for Al-Ti PICC it was 0.9%. TGA studies revealed higher thermal decomposition of saponite clay (38.7%) in comparison to Al-Ti PICC (5.7%).

DTG analysis of saponite clay showed decomposition with weight loss of 0.6 x 10^{-3} mg/sec at 250°C and 0.2 x 10^{-3} mg/sec at 570°C, respectively. While DTG curves of Al-Ti PICC revealed lower weight loss of 0.4 x 10^{-4} mg/sec at 430°C and 0.5 x 10^{-5} mg/sec at 650°C, respectively. Thus, Al-Ti PICC showed lower weight loss in comparison to saponite clay. Thus DTG studies also revealed better thermal stability of Al-Ti-PICC in comparison to sponite clay.

Degradation and Mineralization of 4-nitrophenol over saponite clay

Degradation of 100 mL of 4-NP was studied using 1 g/L of saponite clay. Degradation of 4-nitrophenol using saponite clay was observed to be 10% with mineralization of 1.5% (TOC removal) (Fig. 3). To enhance the degradation and mineralization efficiency, saponite clay was intercalated with Al and Ti metal cations to form Al-Ti PICC. It was found that the surface area of Al-Ti PICC significantly increased in comparison to saponite clay and will significantly enhance the degradation and mineralization of 4-Nitrophenol. The various parameters, such as concentration of H_2O_2, catalyst dose, and temperature that can affect the degradation of 4-NP, have also been optimized using synthesized Al-Ti PICC.

Effect of H_2O_2 dose

H_2O_2 is an oxidizing agent in the degradation process of 4-NP, and the selection of an optimal concentration of H_2O_2 is vital from the practical point of view i.e. the cost of H_2O_2[34, 3]. The effect of H_2O_2 concentration on the degradation of 4-NP over Al-Ti PICC (0.1 g) was examined at 30°C by varying the H_2O_2 concentration from 4 - 20 mM at 5.7 pH. Fig. 4a(i) reveals the lowest degradation rate for 4-NP

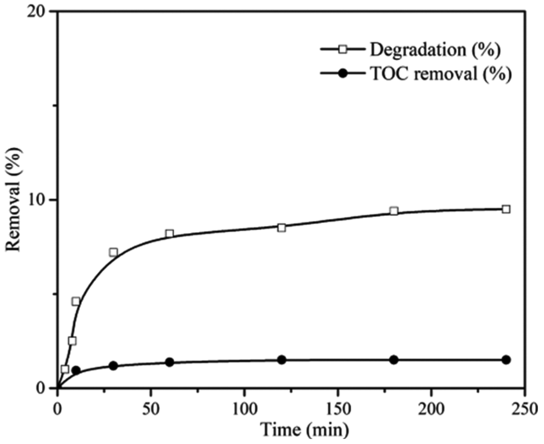

Fig. 3 — Degradation of 4-nitrophenol over saponite clay (100 mg/L 4-nitrophenol, H_2O_2: 4 mM, 1 g/L saponite clay, 5.7 pH and 30°C)

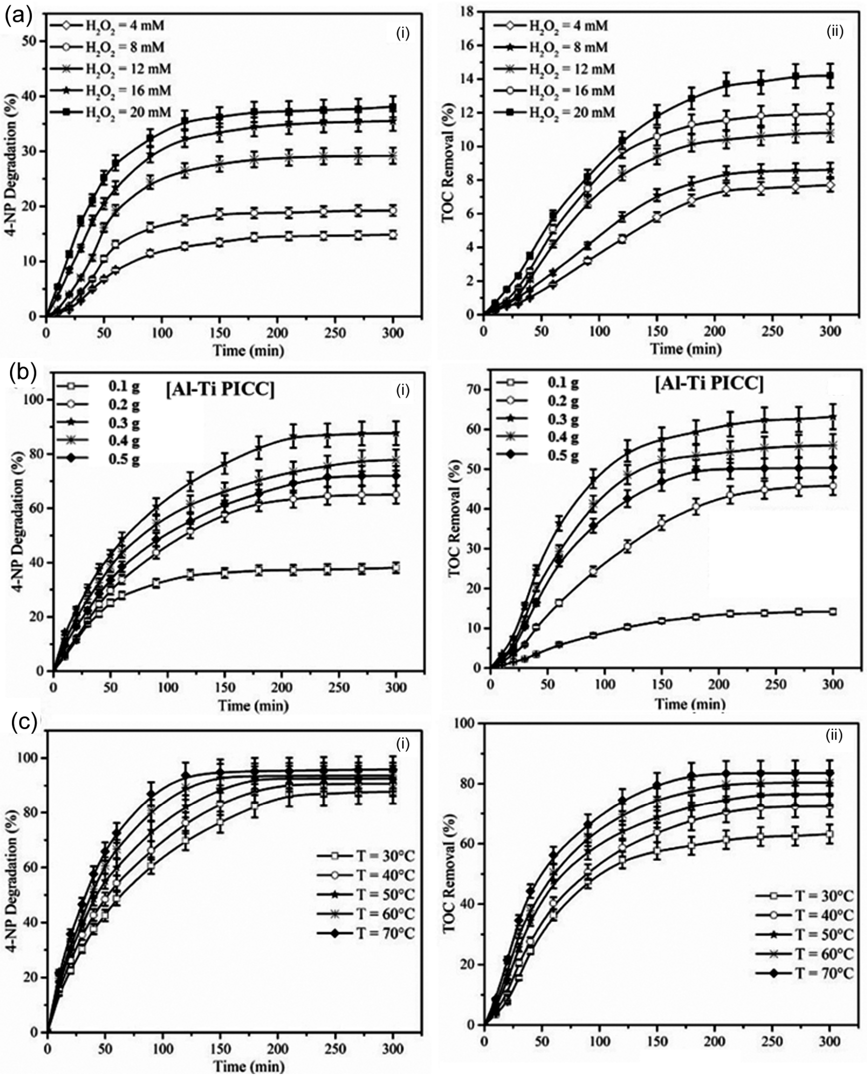

Fig. 4 — (a) Effect of H_2O_2 dose (i) degradation and (ii) TOC removal (100 mg/L 4-nitrophenol in 100 mL, 1g/L of Al-Ti PICC, 30°C), (b) Effect of catalyst (Al-Ti PICC) loading (i) degradation and (ii) TOC removal (100 mg/L 4-nitrophenol, 20 mM H_2O_2, 30°C), pH 5.7 and (c) Effect of temperature (i) degradation and (ii) TOC removal (100 mg/L 4-nitrophenol, 20 mM H_2O_2, 3 g/L of Al-Ti PICC

at 4 mM H_2O_2 dose. The degradation rate for 4-NP was increased by increasing the H_2O_2 dosage from 4 - 20 mM. 4-NP degradation with 20 mM H_2O_2 dose over 0.1 g of Al-Ti PICC was 32.4% after 90 min and was increased to 37.5% after 240 min of reaction time. The mineralization, i.e., TOC removal % with 20 mM H_2O_2 dose, was observed to be 13.8% after 240 min of reaction time (Fig. 4a(ii). The degradation rate increased by increasing the H_2O_2 concentration due to the increase in the production of $HO^{\bullet}$ radicals.

Effect of Al-Ti PICC dose

Al-Ti PICC dosewas varied from 1-5 g/L to examine the effect of catalyst dose on the degradation of 4-NP, and other parameters were kept constant (i.e., 20 mM H_2O_2, 100 mg/L of 4-nitrophenol, 30°C, pH 5.7). It was found that with an increase in Al-Ti PICC dosage from 1 g/L to 3 g/L, the degradation of 4-NP was raised from 37.5% to 87.4% in 240 min. With a further increase in Al-Ti PICC dose from 3 g/L to 5 g/L, the degradation decreased from 87.4% to 71.6% in 240 min (Fig. 4b(i)). Mineralization efficiency at 3 g/L of Al-Ti PICC was found to be 62.8% whereas it was decreased to 50.1% at 5 g/L of Al-Ti PICC dose (Fig. 4b(ii)).

The increment in the degradation of 4-nitrophenol occurred with an increase in catalyst dose because more $HO^{\bullet}$ radicals were available for oxidation reaction[14]. After 3 g/L of catalyst loading, the degradation of 4-NP was reduced due to the scavenging effect of excess iron on $HO^{\bullet}$ radicals.

Effect of temperature

Degradation of 4-NP has also been studied at varying temperatures i.e. from 30 to 70°C and keeping other parameters constant at optimum conditions. Results emphasized that the degradation of 4-NP accelerated with an increase in temperature from 30°C to 70°C (Fig. 4c(i)). The degradation of 4-NP was 87.4% at 30°C and it increased to 95.6% at 70°C after 240 min of the reaction period. The TOC removal efficiency was observed to be 83.4% at 70°C (Fig. 4c(ii)). The enhanced degradation efficiency and TOC removal can be explained due to dependence of rate constant on temperature. Rate of hydroxylation of $HO^{\bullet}$ radicals was increased due to the increase in temperature which might have resulted in higher degradation of 4-NP. The results are in accordance to the studies of Herney-ramirez *et al.* [14] and Ayodele *et al.*[29].

Lumped kinetic model

Mineralization studies of 4-NP using Al-Ti PICC showed 83.4% TOC removal at 70°C after 240 min of the reaction period. The residual TOC of 16.6% remained in the solution due to non-oxidized compounds formed during the degradation of 4-NP. Therefore, the Lumped kinetic (LK) model[33] explains the formation of non-oxidized compounds during the degradation of 4-NP (Eq. 4).

In the LK model, "A" represents 4-NP, "D" as the non-oxidizable compounds generated during the degradation of 4-NP that were persistent in the solution, and "C" is the formation of H_2O and CO_2 after the oxidation of A.

$$A + \bullet OH \xrightarrow{k\prime 1} C \qquad \ldots (3)$$

$$A + \bullet OH \xrightarrow{k\prime 2} D \qquad \ldots (4)$$

The rate expressions involved the TOC contribution of compounds A and D are:

$$-\,r_A = -\,\frac{dC_{TOC_A}}{dt} = (k_1' + k_2')C_{TOC_A} \qquad \ldots (5)$$

$$-\,r_D = -\,\frac{dC_{TOC_D}}{dt} = -\,k_2' C_{TOC_A} \qquad \ldots (6)$$

On integrating Eq. (5) and (6), the expression for TOC concentration with time

$$\frac{C_{TOC}}{C_{TOC_0}} = \frac{C_{TOC_A} + C_{TOC_D}}{C_{TOC_{A0}} + C_{TOC_{D0}}} \qquad \ldots (7)$$

$$\frac{C_{TOC}}{C_{TOC_0}} = \frac{C_{TOC_{D0}}}{C_{TOC_0}} + \frac{C_{TOC_{A0}}}{C_{TOC_0}}\left(\frac{k_2'}{k_1' + k_2'} + \frac{k_1'}{k_1' + k_2'}e^{-(k_1' + k_2')t}\right)$$

C_{TOC_A} and C_{TOC_D} corresponds to the TOC concentration of A and D in time t, $C_{TOC_{A0}}$ and $C_{TOC_{D0}}$ corresponds to the TOC concentration of A and D at the time, t = 0.

As D is absent initially, therefore the Eq. 7 can be simplified by putting $C_{TOC_{D0}} = 0$

$$\frac{C_{TOC}}{C_{TOC_0}} = \frac{C_{TOC_A} + C_{TOC_D}}{C_{TOC_{A0}}}$$

$$\frac{C_{TOC}}{C_{TOC_0}} = \frac{k_2'}{k_1' + k_2'} + \frac{k_1'}{k_1' + k_2'}e^{-(k_1' + k_2')t}\ (8) \qquad \ldots (8)$$

$$\frac{C_{TOC}}{C_{TOC_0}} = a + b * e^{-ct} \qquad \ldots (9)$$

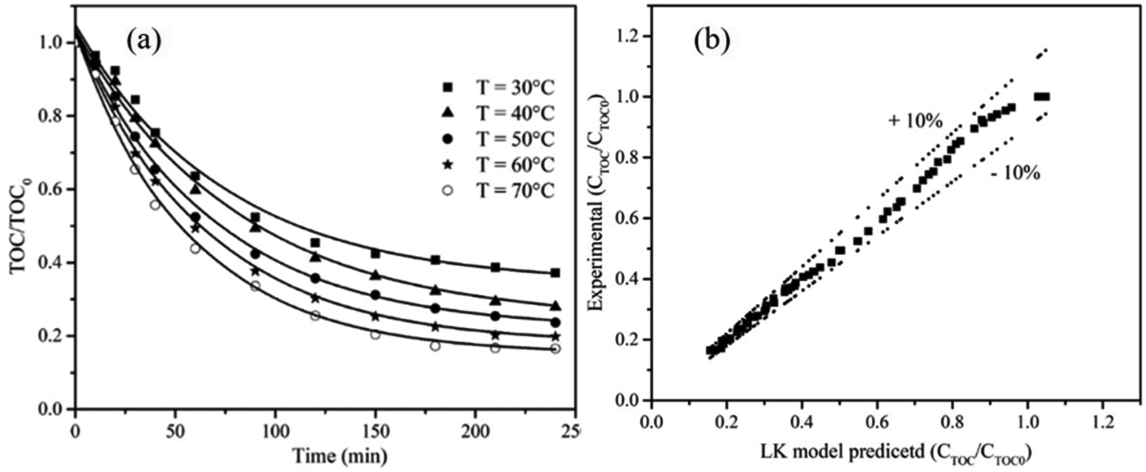

Fig. 5 — (a) validation of LK model for TOC removal of 4-NP at different temperatures (b) Validation of LK model for TOC removal of 4-NP and. Reaction conditions: 100 mg/L of 4-nitrophenol, 20 mM H_2O_2, and 0.3 g/L Al-Ti PICC

Where $a = k'_2/(k'_1 + k'_2)$ is the fraction that reacted into no further oxidizable compounds D,

$b = k'_1/(k'_1 + k'_2)$ is the fraction of initial 4-NP that is oxidized into desired compounds C,

$c = k'_1 + k'_2$ is the overall apparent rate constant for the process.

TOC removal data of 4-NP using Al-Ti PICC was fitted to the LK model at various temperatures i.e 30-70°C. The curve fitting of experimental data of TOC and values predicted using the LK model is presented in Fig. 5(a). The LK model explains the experimental data for TOC removal of 4-NP well at various temperatures (R^2> 0.98). The kinetic parameters were calculated using the non-linear least square Levenberg-Marquardt algorithm and are presented in Table 3. The kinetic parameters obtained from the model showed the increase in apparent kinetic constant k'_1 with temperature rise from 30°C to 70°C whereas k'_2 decreased. The increase in rate constant k'_1 and the decrease in k'_2 suggests that the reaction favours the formation of the oxidized product.

The errors related to the model-predicted data, as compared to the experimental data, were evaluated and are shown in Fig. 5(b) and are found to be in the range of ±10%, which justifies that the LK model appropriately describes the TOC removal of 4-nitrophenol.

Table 3 — Kinetic parameters for the LK model

Temperature (°C)	k'_1 (min^{-1})	k'_2 (min^{-1})	R^2	SSE*
30	0.00971	0.00474	0.9881	0.0074
40	0.00995	0.00307	0.9958	0.0034
50	0.01221	0.00300	0.9959	0.0036
60	0.01367	0.00289	0.9970	0.0028
70	0.01583	0.00274	0.9968	0.0033

*Sum of square error

Conclusion

Aluminium and titanium metal cation-pillared saponite clay, referred to as Al-Ti PICC, was synthesized and characterized. XRD analysis indicated an increased basal spacing compared to pristine saponite clay, while BET studies demonstrated higher surface area and pore volume for Al-Ti PICC. TGA/DTG results revealed enhanced thermal stability of synthesized Al-Ti-PICC in comparison to saponite clay. Under optimized conditions (4-nitrophenol concentration of 100 mg/L, 20 mM H_2O_2, 3 g/L Al-Ti PICC, pH 5.7), 87% degradation and 66.4% mineralization (TOC removal) of 4-nitrophenol were achieved after 90 minutes, increasing to 95.6% and 83.4% after 240 minutes. The TOC removal studies revealed the formation of oxidized and non-oxidizable products and are well described by the Lumped kinetic model. The study highlights the efficacy of saponite-based Al-Ti PICC as a catalyst for 4-nitrophenol degradation, especially noteworthy for its performance under near-neutral pH conditions.

References

1 Patial B, Bansal A, Gupta R & Mittal S K, $BiVO_4$-based heterojunction nanophotocatalysts for water splitting and organic pollutant degradation: A comprehensive review of photocatalytic innovation, *Rev Inorg Chem*, 44 (2024) 495.

2 Zhong Y, Liang X, He Z, Tan W, Zhu J, Yuan P, Zhu R & He H, The constraints of transition metal substitutions (Ti, Cr, Mn, Co and Ni) in magnetite on its catalytic activity in heterogeneous Fenton and UV/Fenton reaction: From the perspective of hydroxyl radical generation, A*ppl Catal B Environ*, 150–151 (2014) 612.

3 Garg R, Gupta R & Bansal A, Photocatalytic degradation of imidacloprid using semiconductor hybrid nano-catalyst: kinetics, surface reactions and degradation pathways, *Int J Environ Sci Technol*, 18 (2021) 1425.

4 Garg R, Gupta R & Bansal A, Degradation mechanism, reaction pathways and kinetics for the mineralization of bisphenol a using hybrid ZnO/graphene oxide nano-catalysts, *Korean J Chem Eng*, 38 (2021) 485.

5 Garg R, Gupta R, Singh N & Bansal A, Characterization and performance evaluation of synthesized ZnO nanoflowers, nanorods, and their hybrid nanocomposites with graphene oxide for degradation of orange G, *Environ Sci Pollut Res*, 28 (2021) 57009.

6 Patial B, Bansal A, Gupta R & Mittal S K, Hydrothermal synthesis of (m-t) $BiVO_4$/g-C_3N_4 heterojunction for enhancement in photocatalytic degradation of imidacloprid, *J Environ Chem Eng*, 11 (2023) 111138.

7 Minz S, Gupta R & Garg S, Mineralization and degradation of 4-Nitrophenol using homogeneous Fenton oxidation process, *Environ Eng Res*, 26 (2021) 1.

8 Jean M, Guélou T E & Fournier J, Catalytic oxidation of phenol by hydrogen peroxide over a pillared clay containing iron Active species and pH effect, *Top Catal*, 33 (2005) 225.

9 Minz S, Garg S & Gupta R, Catalytic wet peroxide oxidation of 4-Nitrophenol over Al-Fe , Al -Cu and Al-Cu-Fe pillared clays, *Indian Chem Eng*, 60 (2017) 1.

10 Minz S, Garg S & Gupta R, Catalytic wet peroxide oxidation of 4-Nitrophenol over Al–Fe PILC: Kinetic study using Fermi's equation and mechanistic pathways based on TOC reduction, *Chem Eng Commun*, 205 (2018) 667.

11 Alejandro L, Ángel M & Gil A, Treatment of municipal leachate of landfill by Fenton-like heterogeneous catalytic wet peroxide oxidation using an Al/Fe-pillared montmorillonite as active catalyst, *Chem Eng J*, 178 (2011) 146.

12 Silva A S, Kalmakhanova M S, Massalimova B K, Sgorlon J G, Diaz-de T J L & Gomes H T, Wet peroxide oxidation of paracetamol using acid activated and Fe/Co-Pillared clay catalysts prepared from natural clays, *Catalysts*, 9 (2019) 1.

13 Catrinescu C, Arsene D & Teodosiu C, Catalytic wet hydrogen peroxide oxidation of para-chlorophenol over Al/Fe pillared clays (AlFePILCs) prepared from different host clays, *Appl Catal B Environ*, 101 (2011) 451.

14 Herney-ramirez J, Silva A M T, Vicente M A, Costa C A & Madeira L M, Degradation of acid orange 7 using a saponite-based catalyst in wet hydrogen peroxide oxidation : Kinetic study with the Fermi's equation, *Appl Catal B Environ*, 101 (2011) 197.

15 Silva A M T, Herney-ramirez J, Söylemez U & Madeira L M, A lumped kinetic model based on the Fermi's equation applied to the catalytic wet hydrogen peroxide oxidation of acid orange 7, *Appl Catal B Environ*, 121–122 (2012) 10.

16 Gao Y, Gan H, Zhang G & Guo Y, Visible light assisted Fenton-like degradation of rhodamine B and 4-nitrophenol solutions with a stable poly-hydroxyl-iron/sepiolite catalyst, *Chem Eng J*, 217 (2013) 221.

17 Kim S & Lee D, Preparation of Al-Cu pillared clay catalysts for the catalytic wet oxidation of reactive dyes, *Catal Today*, 97 (2004) 153.

18 Daud N K & Hameed B H, Acid red 1 dye decolorization by heterogeneous Fenton-like reaction using Fe/kaolin catalyst, *Desalination*, 269 (2011) 291.

19 Zhou S, Zhang C, Hu X, Wang Y, Xu R, Xia C, Zhang H & Song Z, Catalytic wet peroxide oxidation of 4-chlorophenol over Al-Fe-, Al-Cu-, and Al-Fe-Cu-pillared clays : Sensitivity, kinetics and mechanism, *Appl Clay Sci*, 95 (2014) 275.

20 Ts S, Dambueva D V, Ts E, Gil A, Vicente M A & Timofeeva M N, Fenton degradation of sulfanilamide in the presence of Al, Fe-pillared clay: Catalytic behavior and identification of the intermediates, *J Hazard Mater*, 293 (2015) 21.

21 Ayodele O B, Lim J K & Hameed B H, Pillared montmorillonite supported ferric oxalate as heterogeneous photo-Fenton catalyst for degradation of amoxicillin, *Appl Catal A Gen*, 413-414 (2012) 301.

22 Caudo S, Centi G, Genovese C & Perathoner S, Copper-and iron-pillared clay catalysts for the WHPCO of model and real wastewater streams from olive oil milling production, *Appl Catal B Environ*, 70 (2007) 437.

23 Cardona Y & Gil A, TiO_2/Al-PILC catalysts synthesized from a non-conventional aluminum source of aluminum and applied in the photodegradation of organic compounds, *Top Catal*, (2024) 2.

24 Catrinescu C, Teodosiu C, Macoveanu M & Miehe-brendl J, Catalytic wet peroxide oxidation of phenol over Fe-exchanged pillared beidellite, *Water Res*, 37 (2003) 1154.

25 Bel H, Ben M, Elena M & Da P, Photo-fenton oxidation of phenol over a Cu-doped, *CR Chim*, 18 (2015) 1161.

26 Barreca S, Janeth J, Colmenares V, Pace A, Orecchio S & Pulgarin C, Neutral solar photo-Fenton degradation of 4-nitrophenol on iron-enriched hybrid montmorillonite-alginate beads (Fe-MABs), *J Photochem Photobiol A Chem*, 282 (2014) 33.

27 Ma Y, Huang S & Lin J, Degradation of 4-nitrophenol using the Fenton process, *Water Sci Technol*, 42 (2000) 155.

28 Minz S, Gupta R & Garg S, Al-Fe and Al-Ti pillared saponite clay catalysts : Preparation and characterization, *Sustain Eng*, 30 (2019) 37.

29 Ayodele O B & Hameed B H, Synthesis of copper pillared bentonite ferrioxalate catalyst for degradation of 4-nitrophenol in visible light assisted Fenton process, *J Indian Eng Chem*, 19 (2013) 966.

30 Kaneko T, Shimotsuma H, Kajikawa M, Hatamachi T, Kodama T & Kitayama Y, Synthesis and photocatalytic activity of titania pillared clays, *J Porous Mater*, 8 (2001) 295.

31 Mata G, Trujillano R, Vicente M A & Belver C, Chromium-saponite clay catalysts: Preparation, characterization and catalytic performance in propene oxidation, *Appl Catal A: Gen*, 327 (2007) 1.

32 Guerra D L, Airoldi C, Lemos V P & Ang S, Adsorptive, thermodynamic and kinetic performances of Al/ Ti and Al/ Zr-pillared clays from the Brazilian Amazon region for zinc cation removal, *J Hazard Mater*, 155 (2008) 230.

33 Ayodele O B & Hameed B H, Development of kaolinite supported ferric oxalate heterogeneous catalyst for degradation of 4-nitrophenol in photo-Fenton process, *Appl Clay Sci*, 83–84 (2013) 171.

34 Sun J, Sun S, Wang G & Qiao L, Degradation of azo dye Amido black 10B in aqueous solution by Fenton oxidation process, *Dyes Pigm*, 74 (2007) 647.

35 Ramirez J H, Costa C A, Madeira L M, Mata G, Vicente M A, Rojas-Cervantes M L, López-Peinado A J & Martín-Aranda R M, Fenton-like oxidation of Orange II solutions using heterogeneous catalysts based on saponite clay, *Appl Catal B Environ*, 71 (2007) 44.